

RESEARCH PAPER



## *Rhodococcus* spp. interacts with human norovirus in clinical samples and impairs its replication on human intestinal enteroids

Cristina Santiso-Bellón <sup>a,b</sup>, Walter Randazzo <sup>c</sup>, Noelia Carmona-Vicente<sup>a</sup>, Nazaret Peña-Gil <sup>a,b</sup>, Roberto Cárcamo-Calvo <sup>a,b</sup>, Sergi Lopez-Navarro <sup>a,b</sup>, Noemi Navarro-Lleó <sup>a</sup>, Maria J. Yebra <sup>d</sup>, Vicente Monedero <sup>d</sup>, Javier Buesa <sup>a,b</sup>, Roberto Gozalbo-Rovira <sup>a,b</sup>, and Jesús Rodríguez-Díaz <sup>a,b</sup>

<sup>a</sup>Departamento de Microbiología, Facultad de Medicina, Universidad de Valencia, Valencia, Spain; <sup>b</sup>INCLIVA Instituto de Investigación Sanitaria del Hospital Clínico de Valencia, Valencia, Spain; <sup>c</sup>Departamento de Conservación y Seguridad Alimentaria, Instituto de Agroquímica y Tecnología de Alimentos (IATA-CSIC), Valencia, Spain; <sup>d</sup>Departamento de Biotecnología de Alimentos, Instituto de Agroquímica y Tecnología de Alimentos (IATA-CSIC), Valencia, Spain

### ABSTRACT

Viral infections, particularly human norovirus (NoV), are a leading cause of diarrheal diseases globally. To better understand NoV susceptibility, it is crucial to investigate both host glycobiology and the influence of the microbiota. Histo-blood group antigens (HBGA) displayed on surfaces of host cells act as NoV receptors, while certain bacteria express HBGA-like substances, facilitating virus-bacteria interactions. To identify bacterial species interacting with NoV during infection, stool samples from children infected with NoV GII.4 were analyzed. The samples were subjected to bacteria separation using anti-NoV GII.4 polyclonal antibodies coupled to magnetic beads, followed by microbiota profiling through 16S rDNA sequencing. This approach identified the genus *Rhodococcus* as enriched in samples captured with anti-NoV antibodies compared to controls. Electron microscopy confirmed the binding of NoV GII.4 Sydney 2012 viral-like particles (VLP) to five *Rhodococcus* strains from different species, which expressed HBGA-like substances on their surfaces, particularly from A and B blood groups. In human intestinal enteroids, *Rhodococcus erythropolis* reduced NoV GII.4 Sydney 2012 infection levels under displacement, exclusion and competitive exclusion settings. Extracellular polysaccharides (EPS) isolated from *Rhodococcus* strains bound VLP from both GII.4 and GII.6 genotypes. Blocking antibodies targeting A and B epitopes reduced the binding of the EPS from *R. erythropolis* to GII.6 VLP, while enhanced binding to GII.4 VLP was observed when A and B epitopes were blocked. These findings revealed the interaction of *Rhodococcus* to NoV in an *in vitro* setting and open new avenues for developing innovative antiviral strategies to prevent and treat NoV infections through the HBGA-like substances present in their EPS.

### ARTICLE HISTORY

Received 30 July 2024  
Revised 7 February 2025  
Accepted 14 February 2025

### KEYWORDS



Human norovirus; gut microbiota; stool samples; *Rhodococcus*; human intestinal enteroids; histo-blood group antigens


## Introduction

Viral infections are a leading cause of diarrheal diseases and are the second cause of death in developing countries.<sup>1</sup> Among these, human norovirus (NoV) is a predominant etiological agent of acute gastroenteritis (AGE). According to the Center for Disease Control and Prevention, an estimated 685 million cases of NoV infection occur annually, with 200 million of these cases affecting children under the age of 5. NoV-induced fatalities among young children can reach up to 50,000 each year.<sup>2</sup> Moreover, NoV represents the main origin of sporadic outbreaks of gastroenteritis linked to food ingestion, accounting for roughly 50% of

such occurrences globally.<sup>3,4</sup> NoV exhibit high infectivity, with minimal viral loads sufficient to initiate infection. Multiple transmission routes are implicated in NoV AGE, including the consumption of contaminated water and food, person-to-person contact, aerosols exposure, and the fecal-oral route.<sup>5</sup> Phylogenetic analysis of the NoV VP1 protein has revealed significant genetic diversity, with more than 49 genotypes. However, the GII.4 Sydney 2012 variant is responsible for the majority of global NoV outbreaks.<sup>6</sup>

To comprehensively investigate susceptibility to NoV infection, two crucial aspects within the intricate intestinal ecosystem must be addressed. First,

**CONTACT** Jesús Rodríguez-Díaz  [jesus.rodriguez@uv.es](mailto:jesus.rodriguez@uv.es)  Departamento de Microbiología, Facultad de Medicina, Universidad de Valencia, Avenida Blasco Ibañez 15, 46010 Valencia, Spain

 Supplemental data for this article can be accessed online at <https://doi.org/10.1080/19490976.2025.2469716>.

© 2025 The Author(s). Published with license by Taylor & Francis Group, LLC.

This is an Open Access article distributed under the terms of the Creative Commons Attribution-NonCommercial License (<http://creativecommons.org/licenses/by-nc/4.0/>), which permits unrestricted non-commercial use, distribution, and reproduction in any medium, provided the original work is properly cited. The terms on which this article has been published allow the posting of the Accepted Manuscript in a repository by the author(s) or with their consent.

the significance of host glycobiology is paramount. Multiple studies highlight the role of histo-blood group antigens (HBGA) present on mucosal surfaces as receptors for NoV. Furthermore, distinct binding patterns have been observed among various NoV genotypes and variants in relation to different types of HBGA present within the human population.<sup>7–10</sup> Secondly, in recent years, the influence of the intestinal microbiota on the restriction or promotion of NoV infection has been observed.<sup>11–13</sup> Additionally, some bacterial groups, such as *Enterobacter cloacae*, *Enterobacter faecium*, *Klebsiella* spp., *Citrobacter* spp., *Ruminococcus gauvreauii* and *Hafnia alvei* are known to express HBGA-like substances on their surfaces, which participate in the mechanisms of interaction between these bacterial groups and enteric viruses.<sup>14–16</sup>

The historical lack of a consistent human NoV replication model has significantly hindered research into susceptibility to NoV infection. Consequently, much of the evidence to date has been derived from *in vitro* and animal models. Recognizing the emerging role of bacteria in NoV interactions, this study aimed to identify bacterial taxa associated with NoV during natural human infections and evaluate their influence on NoV infectivity using an *in vitro* model. To achieve this, the microbiota associated with NoV was analyzed by 16S rDNA analysis using stool samples from NoV-infected individuals. The investigation further evaluated the relevance of one identified genus, *Rhodococcus*, in NoV interaction and its effects in NoV infection in human intestinal enteroids (HIE), focusing on the likely role of the exopolysaccharides (EPS) they produce.

## Results

### Detection of intestinal bacteria binding to GII.4 Sydney 2012 NoV

Stool specimens obtained from nine children diagnosed with NoV GII.4 Sydney 2012-induced gastroenteritis were subjected to analysis to characterize bacterial genera interacting with the virus in samples derived from human subjects. This task involved cell separation facilitated by magnetic particles and treatments employing two polyclonal antibody (pAb) types (IgG isotype

control and anti-NoV GII.4 Sydney 2012 IgG). Three distinct groups of bacterial populations were obtained: bacteria captured by the IgG isotype control pAb (C), bacteria unreactive to any antibodies (neither the isotype control nor the specific pAb) (N), and bacteria captured by the anti-NoV GII.4 Sydney 2012 pAb (NoV). Subsequently, the microbial composition of each bacterial subpopulations was analyzed by 16S rDNA sequencing and compared to that of the whole microbiota present in the stool samples (total bacteria, T; Supplementary Figure S1). A LEfSe analysis was used to discover microbial taxa characterizing the differences among the different population of these subsamples. This allowed finding 15 taxa exhibiting significant differences ( $p < 0.05$  in Kruskal–Wallis test, adjusted by false discovery rate (FDR)) among the various populations (Figure 1(a)). Of particular significance, one bacterial genus, *Rhodococcus*, attained Linear Discriminant Analysis (LDA) score  $> 3$ , indicating that this taxon was a highly significant biomarker in the dissimilarities between groups. This genus displayed notable differences between the NoV group and the other subpopulations ( $p = 3.6 \times 10^{-4}$ , FDR = 0.002; LDA = 3.18). Among the nine fecal samples analyzed, one was excluded from the analyses following an outlier test, as the abundance of *Rhodococcus* spp. in this sample significantly diverged from the typical data trend across the four analyzed subsamples (C, N, NoV and T subsamples corresponding to each fecal sample). Thus, the NoV subpopulation (bacteria captured by anti-NoV pAb) exhibited abundances 292-, 98- and 31-fold higher for *Rhodococcus* than those of the T, C and N groups, respectively, suggesting interaction of this taxon with NoV in the stool samples (Figure 1(b)). The inspection of the 16S rDNA sequences contributing to *Rhodococcus* enrichment in the bacterial population associated to NoV showed that most of the reads belonged to sequences which shared 100% identity to isolates from the *Rhodococcus erythropolis* Group (*R. erythropolis*, *Rhodococcus qingshengii*, *Rhodococcus baikonurensis* and *Rhodococcus degradans*). The analyses at the species level also identified some defined taxa enriched in NoV subsamples with LDA scores  $> 2$ , such as *Lactobacillus taiwanensis/johnsonii*



(FDR =  $7.7 \times 10^{-4}$ , LDA = 2.34) and *Ligilactobacillus murinus/animalis* (FDR =  $3.5 \times 10^{-5}$ , LDA = 2.35). These bacteria were of particular relevance, as some lactobacilli are considered probiotic microorganisms and, for some

strains, binding to NoV virus-like particles (VLP) had already been reported.<sup>17</sup> However, normalized reads and calculated statistical significance were lower for these taxa (Supplementary Figure S2).

### **Rhodococcus spp. binds NoV GII.4 Sydney 2012 VLP *in vitro***

The discovery of the genus *Rhodococcus* as a microorganism enriched in the NoV-associated bacterial population was unexpected, as no link with NoV infectivity had been previously documented for this genus. Consequently, we investigated the

*in vitro* interaction of five strains of different *Rhodococcus* species with NoV GII.4 Sydney 2012 VLP. The results of the *in vitro* binding experiment of VLP with each of the five *Rhodococcus* species are depicted in Figure 2, where images of negative-stain electron microscopy showing interaction between the *Rhodococcus* strains and NoV VLP are

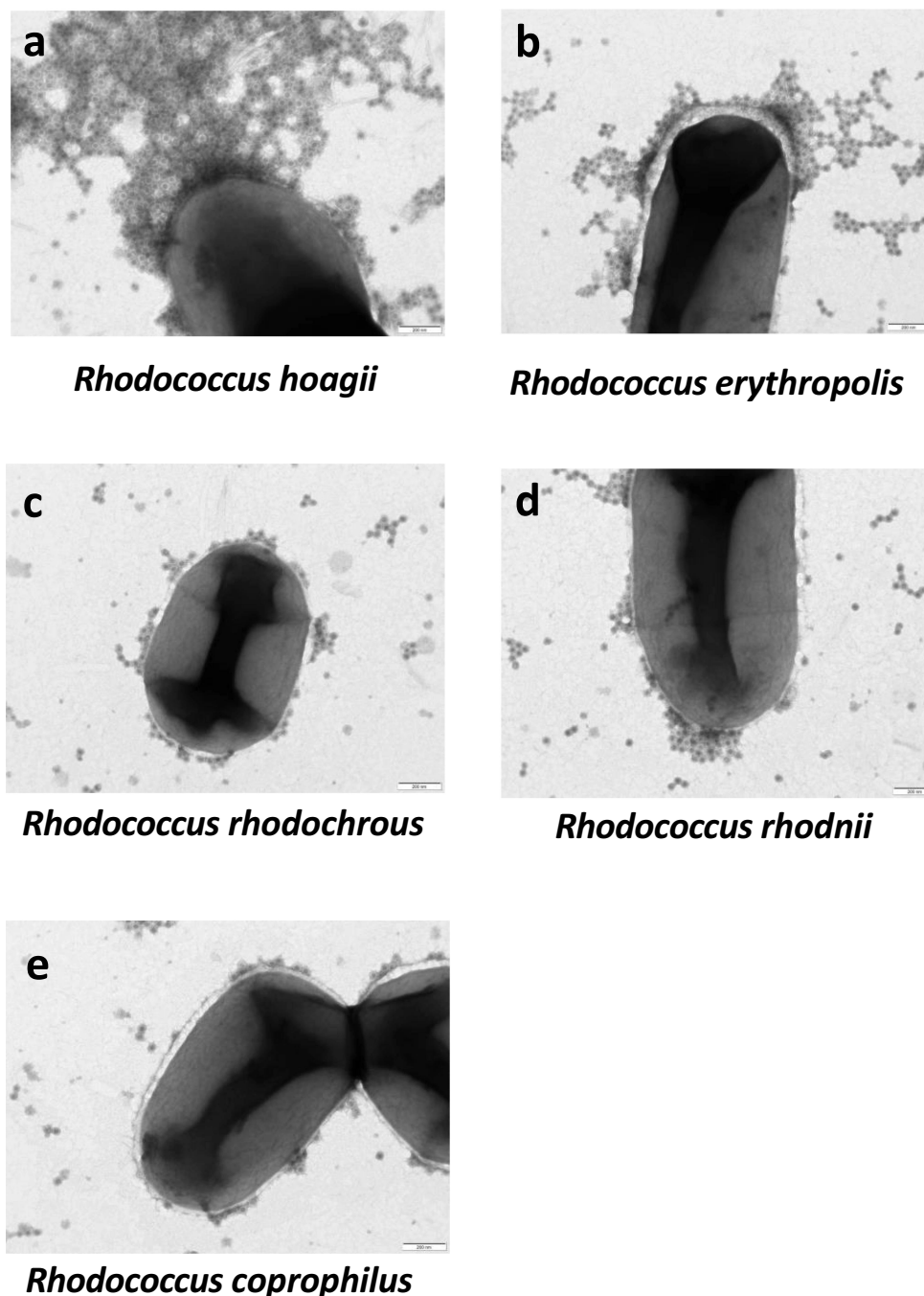


**Figure 2.** Interaction between *Rhodococcus* spp. And NoV GII.4 Sydney 2012 VLP. TEM images with negative staining of the adhesion between (a), *Rhodococcus hoagii*; (b), *Rhodococcus erythropolis*; (c), *Rhodococcus rhodochrous*; (d), *Rhodococcus rhodnii*, and. (e) *Rhodococcus coprophilus* and NoV GII.4 Sydney 2012 VLP (magnification at 21000X). The bars correspond to 200 nm.



presented. Our findings indicate that all five species possess the capability to bind NoV VLP on their surface. This was particularly relevant for species such as *Rhodococcus hoagii* and *R. erythropolis* (Figures 2(a,b)), where VLP were observed aggregating within a mucous-like extracellular substance surrounding the bacterial surface.

### ***R. erythropolis* interferes with NoV infection in intestinal enteroid cultures**

Due to the particular relevance of *R. erythropolis*, we aimed to determine whether this species could exert any effect on NoV infection. This species has also been reported to carry polysaccharides containing fucose.<sup>18</sup> This sugar moiety is present in  $\alpha$ 1,2 linkage configuration in the so-called secretor-positive HBGA, to which NoV GII.4 Sydney 2012 specially interacts.<sup>12</sup> For this purpose, we designed three infection experiments in HIE with *R. erythropolis* CECT3013: displacement (bacteria added after a virus attachment period to HIE), exclusion (virus added to HIE in which bacteria had been previously added), and competitive exclusion (bacteria and virus added simultaneously). In these three experimental settings, the presence of *R. erythropolis* reduced the level of NoV GII.4 Sydney 2012 infection, measured as the increase in the detection of NoV genomes in the HIE cultures, compared to the positive control samples infected with NoV GII.4 Sydney 2012 in the absence of bacteria (Figure 3).

To rule out the possibility that the decrease of infection could be due to any toxicity effect on HIE caused by *R. erythropolis*, HIE were incubated with three different concentrations of bacteria ( $OD_{600} = 0.5$ ,  $OD_{600} = 1$  and  $OD_{600} = 2$ ) for 2 h and the cell monolayer integrity was determined as a measure of toxicity. The results showed that none of the bacterial concentrations impaired monolayer integrity, showing lack of toxicity of the bacteria 24 h after HIE exposure (Supplementary Figure S3).

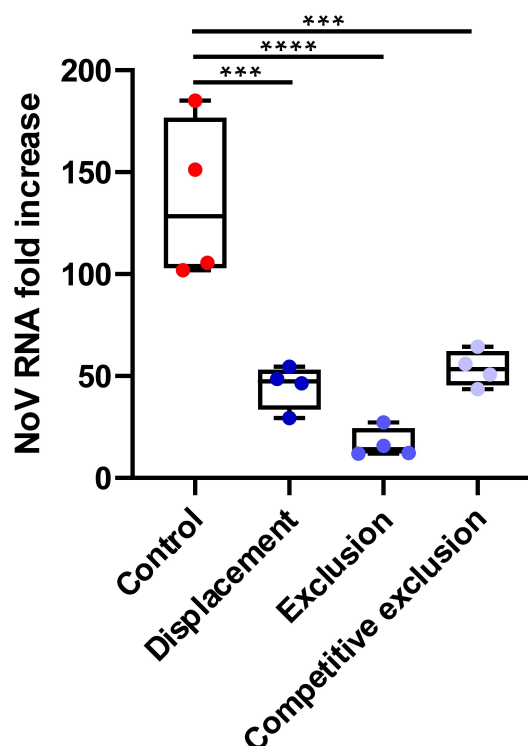


**Figure 3.** Effect of the presence of *R. erythropolis* on NoV infection in HIE. The viral RNA-fold increase from displacement, exclusion and competitive exclusion experiments are shown. In the three experimental settings, *R. erythropolis* ( $OD_{600}$  1) and  $10^4$  genome equivalents of NoV GII.4 Sydney 2012 isolate were added. After 2 h of incubation, the HIE monolayers were washed and NoV infection was let to proceed for further 24 h. Viral RNA was measured by rt-qPCR. \*\*\* $p < 0.001$ , \*\*\*\* $p < 0.0001$  for Sidak's test compared to control without *R. erythropolis* added.

### **Members of the *Rhodococcus* genus exhibit HBGA-like structures on their surface**

As all the *Rhodococcus* species tested were shown to interact *in vitro* with NoV GII.4 VLP, we focused on analyzing whether *Rhodococcus* cells expressed HBGA-like molecules on their surface, which could potentially serve as binding sites between these bacteria and NoV. We evaluated the presence of HBGA-like substances on *Rhodococcus* strains using different HBGA-specific antibodies by ELISA. The assay showed that all strains displayed blood group A, B and Lewis<sup>x</sup>-like substances on their surface (Figures 4(a–e)). As a control, an *E. coli* strain reacted mainly with anti-H antibodies (Figure 4(f)). The strains of *R. erythropolis*, *R. rhodochrous*, *R. rhodnii* and *R. coprophilus* also presented H antigen-like epitopes on their surface (Figures 4(b–e)).

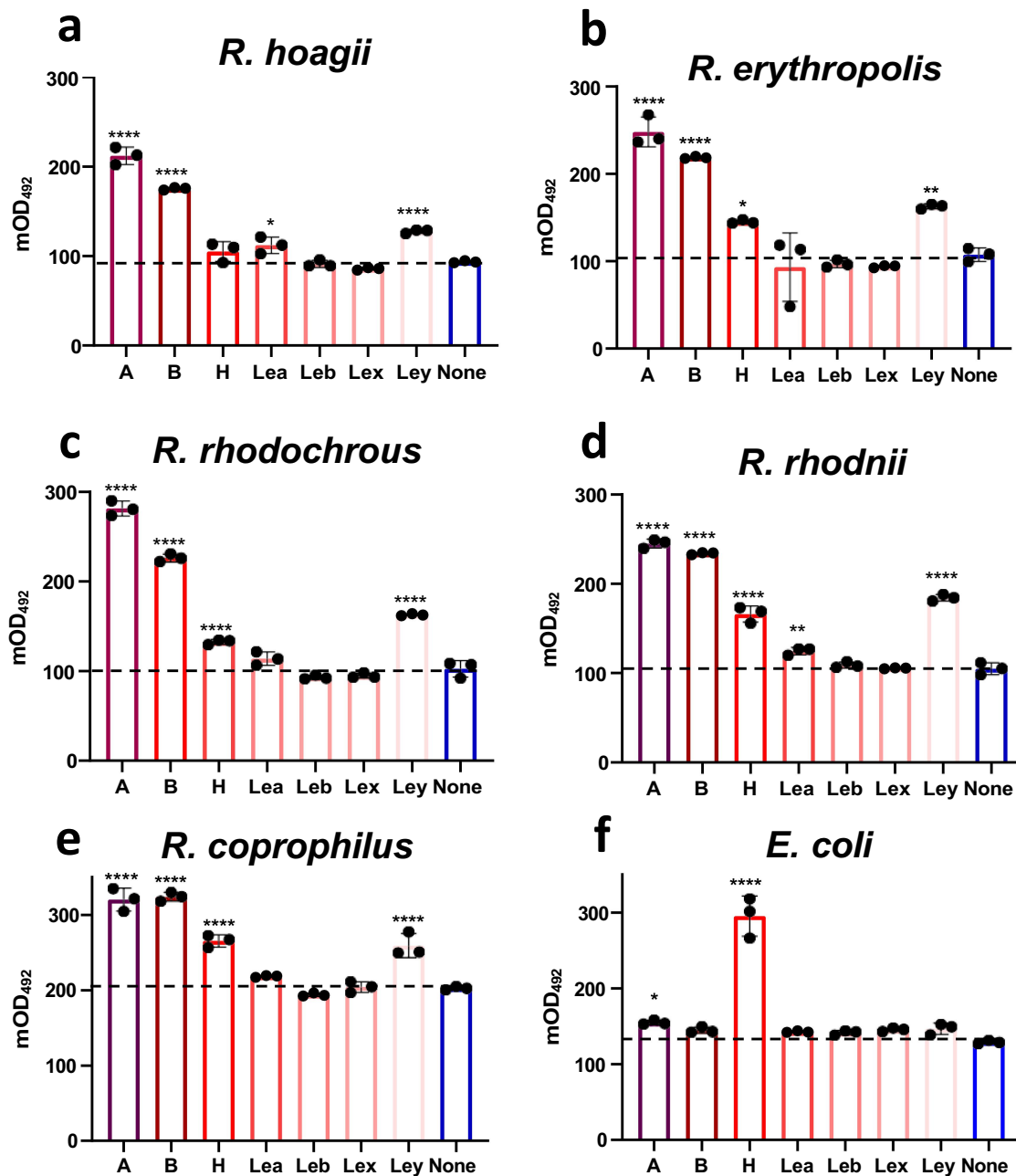


**Figure 4.** *Rhodococcus* spp. express compounds similar to blood group antigens on their surface. The ELISA results of recognition by specific monoclonal anti-hbga antibodies on surface substances of *R. hoagii* (a), *R. erythropolis* (b), *R. rhodochrous* (c), *R. rhodnii* (d), *R. coprophilus* (e) and *E. coli* (f) are shown. The image depicts the mean of triplicates ± SD. Statistical significance is shown with asterisks (\* $p < 0.05$ , \*\* $p < 0.01$ , \*\*\* $p < 0.001$ , \*\*\*\* $p < 0.0001$ ; Sidak's test) for each strain compared to the negative control, "None" (samples incubated only with the secondary antibody anti-mouse HRP).

#### The EPS from members of *Rhodococcus* bind NoV GII.4 Sydney 2012 and NoV GII.6 VLP

Electron microscopy images of NoV GII.4 Sydney 2012 VLP interactions with *Rhodococcus* cells suggested that in some cases, particularly with *R. hoagii* and *R. erythropolis*, VLP aggregated within a mucus-like structure surrounding the

bacterial cells. The apparent viscosity observed in liquid cultures of the employed *Rhodococcus* strains (not shown) suggested that these bacteria were producing extracellular EPS. To investigate whether these EPS were responsible for the observed NoV interactions with *Rhodococcus*, the extracellular polymeric substances were isolated

and tested for their ability to bind NoV VLP. In these experiments, VLP from the NoV GII.6 genotype were also included, as it had previously been demonstrated that this genotype binds to blood group A and B structures present in the EPS of the *Enterobacter cloacae* SENG6 strain.<sup>14</sup> The functionality of both produced VLP (GII.4 and GII.6 genotypes) was confirmed through their interaction with saliva from individuals with specific HBGA phenotypes. These saliva samples contain fucosylated HBGA in the form of glycoconjugates, to which NoV VLP are capable of binding (Supplementary Figure S4). As a negative control, Group A rotavirus (RVA) double-layered particles

(DLP), consisting of the inner and intermediate layers of the rotavirus capsid (VP2 and VP6 proteins) and lacking the outer layer (VP7 and VP4 proteins), were used, as RVA DLP have been shown not to bind HBGA.<sup>19</sup> Figure 5 demonstrates that EPS derived from the five *Rhodococcus* strains bound to both GII.4 Sydney 2012 and GII.6 VLP, but not to the RVA DLP negative control. This finding suggests that the ability of *Rhodococcus* spp. to attach to NoV resides in their EPS. Furthermore, in these experiments, the binding of the different EPS to GII.6 VLP was significantly higher compared to their binding to GII.4 Sydney 2012 VLP ( $p < 0.01$ ).

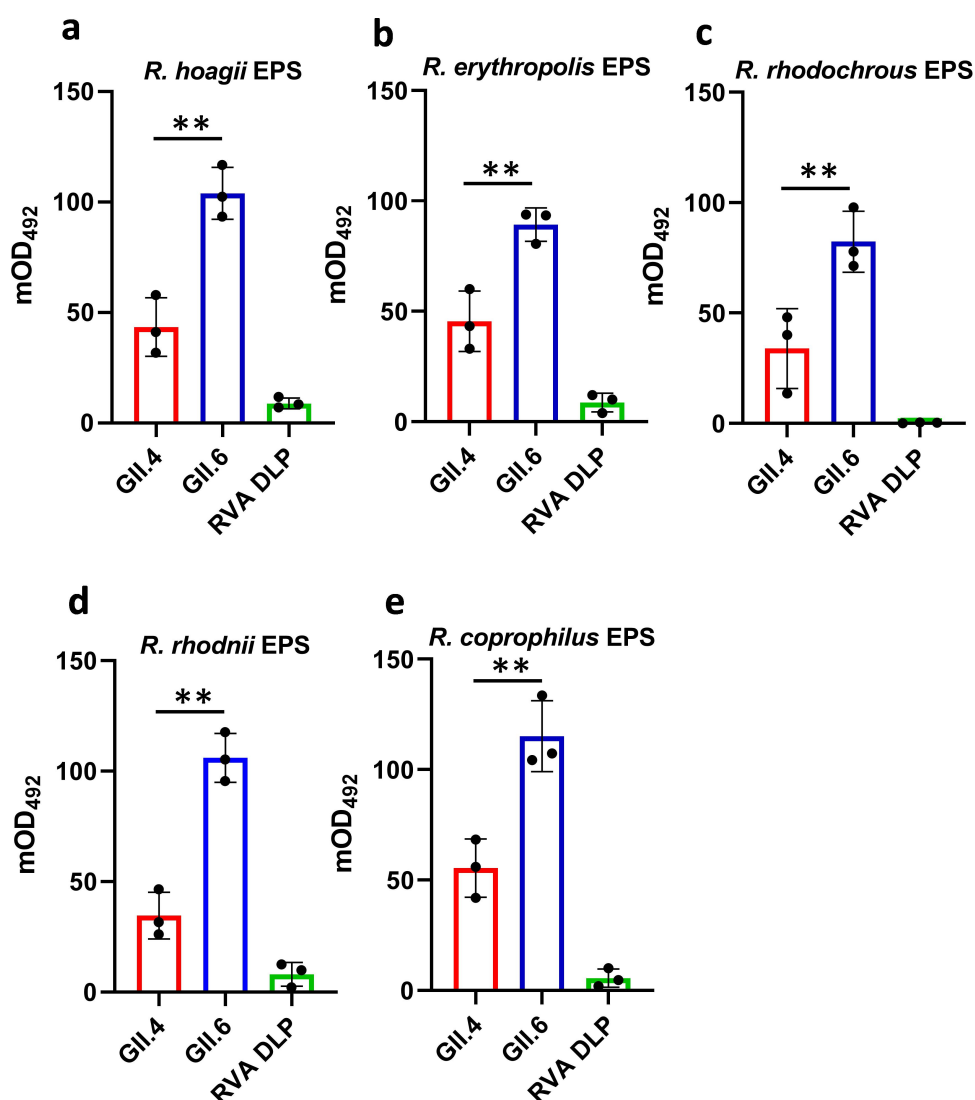


**Figure 5.** The EPS from *Rhodococcus* spp. bind to NoV GII.4 Sydney 2012 and NoV GII.6 VLP. Binding of the five isolated EPS to two NoV VLP (GII.4 Sydney 2012 and GII.6) and to rotavirus a DLP (RVA DLP) is shown. RVA DLP were used as negative control since they do not bind HBGA. Panel (a) shows the binding of *Rhodococcus hoagii*; panel (b), *R. erythropolis*; panel (c), *R. rhodochrous*; panel (d), *R. rhodnii*, and panel (e), *R. coprophilus*. The GII.6 VLP show a significant (\*\* $p < 0.01$ , Student's *t*-test) higher binding to each EPS compared to GII.4 Sydney 2012 VLP.

As blood group A and blood group B-like substances were the more abundant in all assayed *Rhodococcus* strains, and *R. erythropolis* reduced NoV GII.4 Sydney 2012 infection in HIE, a blocking assay with antibodies against these two HBGA was performed in order to detect inhibition in NoV VLP binding to *R. erythropolis* EPS. This EPS was biotinylated for its detection. Biotinylated EPS conserved the same binding pattern than non-biotinylated EPS, showing higher attachment to the GII.6 VLP compared to GII.4 Sydney 2012 ( $p < 0.01$ ) and lack of interaction to RVA DLP (Figure 6(a)). Blocking experiments with anti-A and anti-B antibodies showed a strong reduction of GII.6 VLP binding to the biotinylated EPS ( $p < 0.01$ ), indicating that these antibodies targeted epitopes in the *R. erythropolis* EPS that were recognized by NoV GII.4 VLP (Figure 6(b)). Surprisingly, the presence of the antibodies increased the binding of GII.4 Sydney 2012 VLP to the EPS ( $p < 0.01$ ) (Figure 6(c)).

## Discussion

Since the demonstration that the gut microbiota played a significant role in viral infectivity,<sup>20,21</sup> efforts were made to determine its function for the most relevant viruses causing gastroenteritis, such as rotavirus and NoV.<sup>11</sup> Thus, the gut microbiota has emerged as a key player in the interactions that take place between enteric viruses and the host, and different mechanisms have been shown or hypothesized to confer both positive and negative effects on viral infectivity.<sup>11,22–24</sup> Many studies have demonstrated the interaction of NoV with specific bacterial strains via surface attachment in *in vitro* tests.<sup>14,15,25</sup> However, determining whether this interaction plays a specific role in NoV infectivity remains a challenging task. In this study, we used clinical samples from children with acute diarrhea caused by GII.4 Sydney 2012 NoV, currently the most significant NoV variant,<sup>6</sup> to identify bacterial NoV binders in a real setting.<sup>6</sup> Through the use of immunoseparation with magnetic particles, we identified *Rhodococcus* as bacteria that interacted with GII.4 Sydney 2012 NoV in diarrheal samples.

*Rhodococcus* is a genus of Gram-positive aerobic bacteria widely distributed in nature. It belongs to the phylum *Actinomycetota*, family *Corynebacteriaceae*

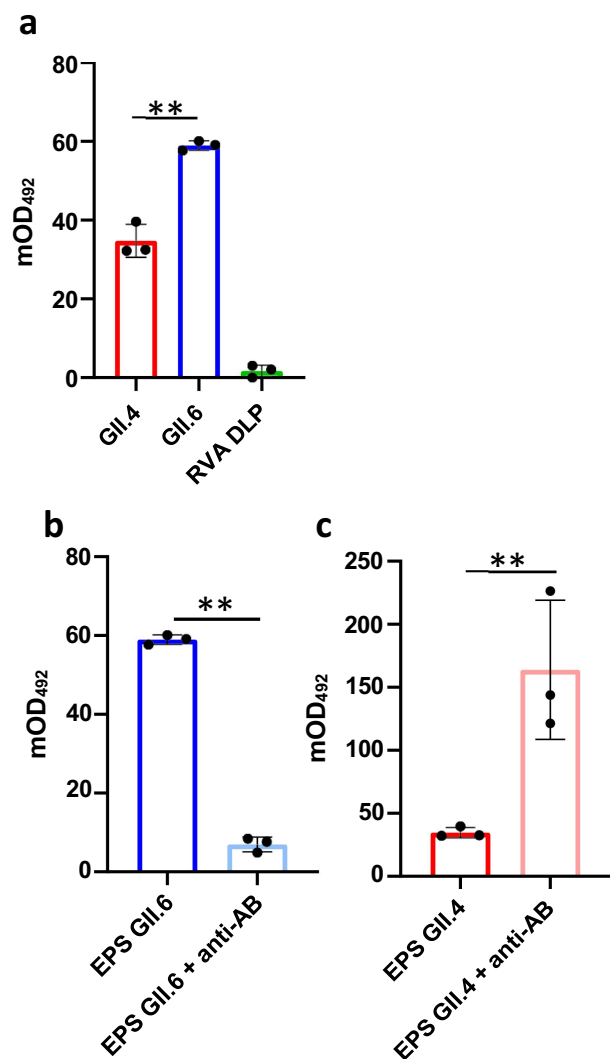


**Figure 6.** Blocking assay by anti-A and anti-B antibodies of *R. erythropolis* EPS binding to NoV VLP. Biotinylated EPS (EPS-Biotin) from *R. erythropolis* was utilized in a binding assay with NoV GII.4 Sydney 2012 and NoV GII.6 VLP. Panel (a) shows that after biotinylation, the EPS still bound specifically to the NoV VLP but not to RVA DLP, being the binding to GII.6 VLP significantly ( $**p < 0.01$ , Student's *t*-test) higher compared to GII.4 Sydney 2012 VLP. Panel (b) shows that anti-A and anti-B antibodies significantly ( $**p < 0.01$ , Student's *t*-test) decreased the binding of the EPS to NoV GII.6. Panel (c) shows that incubation with anti-A and anti-B antibodies significantly ( $**p < 0.01$ , Student's *t*-test) increased the binding of the EPS to NoV GII.4 Sydney 2012.

and it has been isolated from soil, water, and from various living organisms. Some species are known to be pathogenic, such as *R. hoagii* (formerly *Rhodococcus equi*), causing zoonotic infections, and the phytopathogen *Rhodococcus fascians*.<sup>26</sup> In the past decade, species of *Rhodococcus* have attracted considerable interest due to their high catabolic properties. These bacteria can degrade various



contaminants (polycyclic aromatic hydrocarbons, dioxins, dioxin-like polychlorinated biphenyls, etc.), making them useful for soil bioremediation.<sup>27</sup> Despite being an aerobic microorganism, *Rhodococcus* can be detected in human stool samples.<sup>28,29</sup> Whether this bacterium interacts with NoV in the colon or is present in the small intestine, where NoV replicates, and is subsequently detected in fecal samples, remains to be determined through further analysis.

Limited information is available regarding potential links between *Rhodococcus* and NoV infectivity. A recent study involving immunocompromised children infected with NoV observed differences in intestinal bacterial composition compared to immunocompetent children. The results revealed that the microbiota of immunocompromised children showed an increased abundance of various taxa, including members of the *Corynebacteriaceae* family such as *Rhodococcus*.<sup>30</sup> However, whether this observation holds any relevance to NoV infection remains unknown. Previous experiments with probiotic strains (*Lactocaseibacillus paracasei* and *E. coli* Nissle 1917) with capacity to bind NoV GI.1 P-particles showed that the presence of these bacteria hampered binding of GI.1 particles to HT-29 intestinal cells monolayers in competitive exclusion assays, whereas the bacteria promoted GI.1 particles binding to cells in exclusion or displacement assays.<sup>31</sup> We demonstrated that the five selected species of *Rhodococcus* bound to NoV GII.4 Sydney 2012 VLP. In addition, *R. erythropolis* reduced NoV GII.4 Sydney 2012 infection levels in HIE in three experimental settings (competitive exclusion, exclusion and displacement). The use of this HIE model provides a more realistic situation for studying NoV pathogenicity, as not only host cell binding is considered and viral replication can be achieved. However, the biological relevance of the *in vitro* detected NoV inhibition is still unknown.

All five *Rhodococcus* strains, including *R. erythropolis*, showed recognition by anti-HBGA antibodies against types A and B, and to a lesser extent by anti-H and anti-Le<sup>y</sup> antibodies. These HBGA belong to the secretor pathway, which is determined by the activity of the FUT2 enzyme responsible for adding  $\alpha$ 1,2 fucosyl linkages to their structures. It is widely recognized that NoV

GII.4 Sydney 2012 has a broad binding affinity for HBGA, particularly for secretor HBGA.<sup>12</sup> In a study with purified EPS from *E. cloacae* SENG6, it was determined that NoV GI.1 VLP (recognizing types A and H HBGA)<sup>8,10</sup> bound to type A sugars present in the EPS of this bacterium. Removal of the terminal *N*-acetyl-galactosamine residues (present in antigen A) from this EPS, weakened the binding.<sup>14</sup> Recent studies have characterized the composition of the EPS of some *Rhodococcus* strains, including *R. erythropolis*,<sup>18,32,33</sup> and have determined that it consists in a heteropolysaccharide composed of glucose, galactose, fucose, mannose and glucuronic acid, which are sugar moieties also found in HBGA. Interaction of NoV to bacterial EPS has also been described in other contexts. Most NoV outbreaks involve the consumption of contaminated seafood<sup>34</sup> and recent studies identified the EPS produced by *Pseudomonas composti* as a factor promoting stability/persistence of NoV associated to oysters.<sup>35</sup> Likewise, HBGA substances displayed on surface EPS from *Sphingobacterium* had an impact on the survival of NoV on leafy greens.<sup>25</sup> Therefore, we hypothesized that the binding of NoV VLP to *Rhodococcus* spp. may involve EPS substances produced by these microorganisms. This idea was confirmed by purifying the EPS produced by *Rhodococcus* strains and demonstrating their interaction with NoV VLP. Specifically, GII.6 VLP recognized A and B epitopes in the *R. erythropolis* EPS. Interestingly, the divergent results obtained in blocking experiments with anti-HBGA antibodies might be explained by the distinct recognition of *R. erythropolis* EPS sugar epitopes by GII.4 and GII.6 VLP. While studying galectin-3 recognition of group A and B glycans, it was observed that the presence of certain sugar residues, that do not participate in binding but promoted rigidity, resulted in enhanced molecular recognition.<sup>36</sup> A similar process might be taking place here. While GII.6 VLP recognize the same epitopes on the EPS as anti-blood group antibodies, GII.4 Sydney 2012 VLP might recognize different epitope(s) whose flexible glycan structures can be stabilized by the action of anti-HBGA antibodies, thereby increasing the affinity of GII.4 VLP.

Different studies have evidenced the participation of molecules present in the intestinal

environment in enteric viruses infectivity. It was observed how hydrophobic bile acids induce the accumulation of NoV viral particles near cells, grouping virions and allowing for direct and efficient binding to target cells.<sup>37</sup> Other works with the enterovirus poliovirus showed that bacterial lipopolysaccharide favored the stability of the virion structure and promoted its binding to the surface of target cells.<sup>38</sup> In our case, we postulate that direct binding of NoV to *Rhodococcus* cells via their EPS, and subsequent inability of these sequestered viruses to infect their target cells, may be the main mechanism for viral infectivity restriction in our *in vitro* experiments with HIE. This likely mechanism may be driven by NoV binding to HBGA-like substances present on the bacterial surface, such as their associated EPS. Nevertheless, it remains unclear whether this observation holds significance during NoV infection *in vivo*. Furthermore, other mechanisms cannot be excluded. In this regard, it is interesting to note that substances present in the surface of *Rhodococcus* strains or that form part of their EPS have been shown to possess antiviral activity in some models. In a study with influenza virus, it was demonstrated that a component on the surface of *R. hoagii* (*R. equi*), phosphatidylinositol carrying a branched-chain fatty acid, bound to the viral hemagglutinin and blocked infection of MDCK cells.<sup>39</sup> However, our observations remain insufficient to establish a definitive role for *Rhodococcus* in modulating NoV infectivity. The conclusions drawn from the observed *in vivo* interactions and the *in vitro* results must be interpreted with caution. For instance, previous studies on *E. cloacae* showed that while surface components of this bacterium promoted NoV replication in cultured cells,<sup>40</sup> administering *E. cloacae* in a gnotobiotic pig model inhibited NoV infection.<sup>41</sup> This underscores the need for more clinical data, including comprehensive studies on the presence of *Rhodococcus* and its potential correlation with susceptibility to NoV infection in humans, to determine whether *Rhodococcus* plays any role in NoV infectivity. Furthermore, additional trials using *Rhodococcus* strains in *in vivo* infection models with NoV are essential.

*Rhodococcus* is a versatile genus of bacteria with high potential for biotechnological uses, as its EPS

has been demonstrated to have applications in the food industry (due to its high viscosity),<sup>33</sup> pharmaceutical (antiviral effect) and environment (bioremediation)<sup>27</sup> fields. In this work, we described an interaction of these bacteria with NoV in stool samples, possibly linked to their EPS substances. Whether this fact has a biological relevance in the interplay between bacteria, host and NoV and its effect in the progress of NoV infection in humans deserves further analyses. Nonetheless, the *in vitro* observation that certain *Rhodococcus* species, such as *R. erythropolis*, may exhibit potential antiviral activity against NoV warrants further investigation. This finding could open new avenues for exploring antiviral strategies for the prevention and treatment of NoV infections.

## Material and methods

### NoV detection and genotyping

Stool samples were collected from pediatric patients, with an average of  $14.50 \pm 5.26$  months of age, admitted to the Hospital Clínico Universitario de Valencia between 2015 and 2019. Nine stool samples, which tested positive for GII.4 Sydney 2012 NoV variant by RT-PCR,<sup>42–44</sup> were selected and stored at  $-80^{\circ}\text{C}$  for further analysis.

### Expression and purification of VLP in Sf9 insect cells

The expression of VLP was conducted in suspension culture using Sf9 insect cells (*Spodoptera frugiperda*), following the guidelines outlined in the Bac-to-Bac® Baculovirus Expression Systems (Invitrogen), with some modifications. Synthetic genes (optimized for expression in insect cells using Thermo Fisher Scientific's GeneArt technology) were synthesized based on coding sequences for VP1 (ORF2) and VP2 (ORF3) selected from a clinical strain (Genbank accession number MN248513.1) for the NoV GII.4 VLP. The VP1 and VP2 genes from accession number MN248514.1, were synthesized for producing GII.6 VLP. Each of these genes was cloned into the pFastBac 1 vector (Thermo Fisher Scientific), and the plasmids were transformed into competent *E. coli* DH10Bac cells. The viral stock of VP1 and VP2 was amplified

by infecting a 30-ml suspension of *Sf9* cells at a concentration of  $3 \times 10^6$  cells/ml at a multiplicity of infection (moi) of 0.1. The cells were maintained in SF900 SFMII medium (Thermo Fisher Scientific) supplemented with antibiotics and 1% Pluronic F-127 (Sigma-Aldrich, St. Louis, MO) in culture flasks with aeration at 120 rpm and 27°C. The amplification of each baculovirus was carried out for 5 days. The baculoviruses expressing the VP2 and VP6 genes from the group A rotavirus (RVA) SA11 strain (G3P[2]) were kindly provided by Dr. Daniel Luque from Instituto de Salud Carlos III, Madrid, Spain.

For the production of all the VLP (NoV GII.4 (VP1 + VP2), NoV GII.6 (VP1 + VP2) and RVA (VP2 + VP6), a volume of 500 ml of a cell suspension at  $3 \times 10^6$  cells/ml were infected with a mixture of VP1 and VP2 or VP2 and VP6 baculoviruses in equal proportion, resulting in a final moi of 1 (baculovirus/cells). Production of the VLP was carried out for 5 days. 500 ml of the cell suspension were centrifuged at  $1,000 \times g$  for 10 min at 4°C using a R7A-4007 rotor in a Himac CR-30N centrifuge (Eppendorf Himac Technologies Co.) to remove cellular debris. Subsequently, the supernatant containing the VLP and baculoviruses was centrifuged at  $100,000 \times g$  for 1 h at 4°C using a Himac R25ST-0507 rotor to pellet the viruses. The VLP-containing supernatant was gently agitated overnight at 4°C with 15% polyethylene glycol 8000 and 0.3 M NaCl to aggregate the particles, followed by centrifugation at  $10,000 \times g$  for 30 min at 4°C using a Himac R16A2 rotor to precipitate them. The resulting precipitate was resuspended in 22 ml of 1X filtered PBS (0.22 µm) and supplemented with 1% Triton<sup>TM</sup> X-100, 3.6 U of DNase I, and 1 mM of protease inhibitor phenylmethanesulphonyl fluoride (all from Sigma-Aldrich, St. Louis, MO). This mixture was gently agitated for 30 min at room temperature and then subjected to ultracentrifugation at  $197,000 \times g$  for 12 h at 4°C using a SW41 rotor in an L8-M ultracentrifuge (Beckman Coulter Inc.). The sediment was rehydrated with 2 ml of 1X PBS overnight at 4°C. Finally, after gentle resuspension, it was centrifuged for 5 min at  $15,000 \times g$  in an Eppendorf microcentrifuge. The soluble VLP in the

supernatant were kept at 4°C until use. The purification quality was analyzed by 12% SDS-PAGE, stained with Coomassie blue, and quantified at an absorbance of 280 nm using a NanoDrop<sup>TM</sup> 2000 spectrophotometer (Thermo Fisher Scientific).

### **Production and purification of pAb**

The antibodies were obtained from the serum of female C57BL/6J mice acquired from Charles River Laboratories (Saint Germain Nuelles, France). Blood samples were collected from the lateral saphenous vein, and the antibodies were purified from the serum. Two groups of IgG antibodies were obtained: isotype control IgG antibodies from the serum of non-immunized mice and IgG antibodies against NoV GII.4 Sydney 2012 VLP following three rounds of immunization with previously obtained VLP. Immunization with VLP was performed every 15 days by subcutaneous injection of 100 µl of a mixture consisting of 10 µg of VLP diluted in 100 µl of 1X PBS and 100 µl of 2% Alhydrogel<sup>®</sup> adjuvant (InvivoGen, San Diego, California, USA). Both antibodies were purified using a HiTrap Protein G HP column with the ÄKTA start chromatography system (Cytiva), following the manufacturer recommendations. In summary, 200 µl of each serum were centrifuged for 15 min at  $10,000 \times g$  and 4°C in an Eppendorf microcentrifuge, and the supernatant was mixed with 800 µl of binding buffer (1.5 M glycine, 3 M NaCl at pH 9.0). After equilibrating the entire system with this buffer, the serum sample was injected and passed through the column at a flow rate of 1 mL/min. Antibodies bound to the column were eluted with elution buffer (0.1 M glycine-HCl pH 2.7) and collected in 1 ml fractions with 100 µl of 1 M Tris at pH 8.0 to neutralize the acidity of the elution buffer. The fractions containing IgGs were evaluated through SDS-PAGE. They were analyzed on a 10% polyacrylamide gel under non-reducing conditions to visualize a single band at 150 kDa, corresponding to the complete pAb (two light chains of 25 kDa each plus two heavy chains of 50 kDa). Purified IgGs were also subjected to reducing conditions by electrophoresis on a 15% gel to observe the light chain and heavy chain separately. Finally, the corresponding pAb-containing

fractions were combined, and concentration was achieved through 10 min centrifugations at  $5,000 \times g$  using TS.5.1–500 rotor and Amicon Ultra-4 tubes with 30 K cellulose filters (Merck Millipore, Massachusetts, USA). During the concentration process, a buffer exchange to 1X PBS was performed. The final concentration of each pAb was measured using the Bradford method. The specificity of the IgG pAb against NoV GII.4 Sydney 2012 VLP was assessed by Western blotting against strains of GII.4 Sydney 2012 NoV. The NoV GII.4 Sydney 2012 VLP used for mouse immunization served as a positive control.

### **Isolation of microbiota from faeces**

To detect bacteria that bind to NoV, a similar strategy to that used to quantify the *in vitro* binding of NoV VLP to intestinal commensal bacteria by flow cytometry was followed.<sup>45</sup> Four bacterial populations from each of the nine selected fecal samples were analyzed: total bacteria isolated before treatments (T), bacteria recognized by the IgG isotype control pAb (C subpopulation), bacteria not recognized by the IgG isotype control pAb or the specific pAb (N subpopulation), and bacteria recognized by the anti-VLP IgG pAb of GII.4 Sydney 2012 NoV (NoV subpopulation). Immunoseparation with magnetic particles was used for obtaining the different subpopulations, utilizing the commercial Pierce® MS-compatible Magnetic IP Kit – Protein A/G (Thermo Fisher Scientific).

Two hundred milligrams of each selected fecal sample were weighed and suspended in 1 ml of saline solution (SS, 0.9% NaCl), previously filtered through a 0.22- $\mu$ m filter. They were then gently vortexed at low rpm for 10 s. Subsequently, the suspension was centrifuged at  $2,000 \times g$  for 2 min to remove cellular debris. Bacteria in the supernatant were pelleted at  $12,000 \times g$  for 5 min and subjected to two washes with 1 ml of SS. After the second wash, the bacterial pellet was resuspended in 300  $\mu$ l of SS and fixed overnight at 4°C with 1200  $\mu$ l of 4% paraformaldehyde. After three 5-min washes at  $12,000 \times g$  with 1 ml SS, the bacteria were resuspended in 1 ml of SS. From this 1 ml aliquot of fixed bacteria, 200  $\mu$ l

was set aside, representing the total bacteria (T). The remaining 800  $\mu$ l were centrifuged at  $12,000 \times g$  for 5 min, and the pellet was resuspended in 150  $\mu$ l of SS with blocking solution (5% BSA and 2  $\mu$ g of IgG isotype control antibody obtained previously). This mixture was incubated for 1 h at 37°C and kept overnight at 4°C. Subsequently, 25  $\mu$ l of magnetic particles coated with anti-mouse IgG were added and maintained for 1 h at room temperature with rotation on an Intelli-Mixer™ RM-2 L (ELMI, California, USA) at 95 rpm with program C1. Next, magnetic particles were placed in a DynaMag™-2 device (Thermo Fisher Scientific). The bacteria separated in this step were those recognized by the IgG isotype control antibody (C). Then, the supernatant was incubated for 1 h at 37°C with 2  $\mu$ g of the anti-VLP (GII.4 Sydney 2012) IgG antibody under rotation. After this time, bacteria bound to the magnetic particles (bacteria with bound NoV, NoV) were separated and resuspended in 100  $\mu$ l of SS. The remaining supernatant was centrifuged at  $12,000 \times g$  for 5 min, and the pellet (bacteria not recognized by the IgG isotype control antibody and the specific NoV antibody, N) was resuspended in 100  $\mu$ l of SS.

### **DNA extraction and 16S rDNA sequencing**

Total DNA was isolated using the Masterpure™ DNA Purification Kit (Epicentre Technologies Corporation, Madison, USA) following the method described by Gozalbo-Rovira et al.<sup>16</sup> One hundred microliters of each sample were incubated for 40 min at 37°C with lysis buffer (300  $\mu$ l of Mastermix Tissue and Cell Lysis solution, 1  $\mu$ l of 10 U/ml mutanolysin, and 2  $\mu$ l of 20 mg/ml lysozyme). Subsequently, samples were mixed in a 2-ml screw-capped tube with 0.5 ml of glass beads (0.1 mm diameter) and lysed using the FastPrep-24™ 5 G bead beater apparatus (MP Biomedicals Germany GmbH, Eschwege, Germany) with two cycles of 1.5 min. Then, 2  $\mu$ l of 18.5 mg/ml proteinase K (Roche, Basel, Switzerland) was added, and samples were incubated for 20 min at 65°C with agitation every 5 min. After cooling on ice, they were mixed with 1  $\mu$ l of 5 mg/ml RNase A and incubated for 60 min at 37°C. It was cooled again and mixed for 10 s on a vortex with 155  $\mu$ l of the



protein precipitation reagent from the kit. After centrifugation at  $16,000 \times g$  for 10 min, the supernatants were incubated and mixed with 500  $\mu$ l of isopropanol. DNA was precipitated for 10 min at  $16,000 \times g$ , followed by ethanol washing. After air drying, DNA samples were resuspended in 50  $\mu$ l of MilliQ® water. DNA concentration was measured and normalized using the Qubit® 3.0 fluorometer (Life Technologies, Carlsbad, CA, USA). The extracted DNA was stored at  $-20^{\circ}\text{C}$  until use.

The V3-V4 region of the bacterial 16S rDNA gene was amplified by PCR utilizing Illumina adapter overhang nucleotide sequences as per Illumina protocols. Subsequently, a multiplexing step was carried out with the Nextera XT Index kit (Illumina, San Diego, CA, USA). Amplicons underwent assessment with a Bioanalyzer DNA 1000 chip, and libraries were subjected to sequencing via a  $2 \times 300$  bp paired-end run (MiSeq Reagent kit v3) on a MiSeq-Illumina platform (SCSIE, Universitat de Valencia, Valencia, Spain).

### Bioinformatic analysis

The data were demultiplexed using Illumina's bcl2fastq program. The reads were quality-checked, had their adapters trimmed, and were filtered using AfterQC and FastQC v0.11.8 tools (<http://www.bioinformatics.babraham.ac.uk>).

Filtered reads were checked for chimeric sequences, and non-chimeric sequences were processed using QIIME™ V1.9.1. Chimeric sequences were removed from the reads using the USEARCH 6.1 algorithm. The resulting sequences were clustered at 97% identity into operational taxonomic units (OTUs) using the UCLUST classifier, and taxonomic classification of representative sequences was performed based on the Greengenes 16S rRNA database (version 13.8) using PyNAST.

Microbiome analysis was performed with the Marker Gene Count Data Analysis option of the MicrobiomeAnalyst pipeline (<https://www.microbiomeanalyst.ca/>).<sup>46</sup> A further filtering step was performed to remove low-quality or non-informative features in order to enhance subsequent statistical analysis. Firstly, OTUs with more than two reads were included (6382 of 8391 total OTUs). The data were normalized by rarefying to the minimum library size (188955 of 20,387,750

total reads), and data was scaled to the total sum of squares.

For the identification of bacteria interacting with viruses, LDA Effect Size (LEfSe) was performed.<sup>47</sup> Differences in abundance between virus-binding and non-virus-binding groups were analyzed, focusing on genera with significant differences among the various treatments [ $p < 0.05$  in the Kruskal–Wallis test, adjusted for FDR]. For conducting interaction experiments, the bacterial genus with the highest LDA score was considered.

### Bacterial strains and culture conditions

Five strains representing type species of the genus *Rhodococcus* were obtained from the Spanish Type Culture Collection (CECT, Burjassot, Spain). The bacteria were cultured under aerobic conditions (agitation at 200 rpm) following the recommendations of the CECT: *R. hoagii* CECT555 (TSA medium at  $30^{\circ}\text{C}$ ), *R. erythropolis* CECT3013 (YEME medium at  $30^{\circ}\text{C}$ ), *R. rhodochrous* CECT5749 (YEME medium at  $30^{\circ}\text{C}$ ), *R. rhodnii* CECT5750 (TSA medium at  $26^{\circ}\text{C}$ ) and *R. coprophilus* CECT5751 (YEME medium at  $30^{\circ}\text{C}$ ).

### Binding assays between bacteria and Nov GII.4 Sydney 2012 VLP

The cells of each *Rhodococcus* strain were grown overnight washed and diluted to an  $\text{OD}_{600} = 1$ . Subsequently, 200  $\mu$ l of the bacterial suspension were incubated with 10  $\mu$ g of NoV GII.4 Sydney 2012 VLP for 1 h at  $37^{\circ}\text{C}$  with rotation at 36 rpm. After this period, the suspension was centrifuged and washed twice with 1X PBS at  $2,000 \times g$  for 10 min.

Visualization of the NoV-bacteria interaction was performed through transmission electron microscopy (TEM) at the Electron and Confocal Microscopy Unit of the Carlos III Health Institute (Madrid, Spain) and at the Electron Microscopy Unit of Centro de Investigación Príncipe Felipe (Valencia, Spain). After the final washes to remove unbound VLP, the pellets containing the bacteria were resuspended in 100  $\mu$ l of 1X PBS. 15  $\mu$ l of these suspension were collected and incubated on copper grids coated with collodion-carbon. These grids were previously ionized by ion discharge in



the Quorum Q150T ES system (Quorum Technologies, East Grinstead, United Kingdom). After 5 min of incubation on the grid, two successive washes were performed using 50  $\mu$ l of MilliQ water. Finally, the sample were stained for 1 min with 5  $\mu$ l of 2% (w/v) uranyl acetate. For sample observation, a FEI Tecnai 12 electron microscope equipped with a LaB6 filament was used, operating at 120 kV and equipped with a FEI Ceta CCD camera. Images were captured at a nominal magnification of 21000X.

### **Expression of HBGA-Like substances on the *Rhodococcus* spp. surface**

The different *Rhodococcus* species and *E. coli* DH10B (grown in LB) were grown and adjusted to an OD<sub>600</sub> of 1 in carbonate/bicarbonate buffer.<sup>48</sup> An ELISA plate (Costar) was coated in triplicate with 100  $\mu$ l/well of this bacterial suspension at 4°C overnight. After three washes with PBS-T, the plate was blocked for 1 h at 37°C with 3% BSA in PBS-T. Three additional washes were performed, and the plate was incubated for 1 h at 37°C with monoclonal antibodies against HBGA (anti-blood group A [catalog no. 70501 Diagast], anti-blood group B [catalog no. 70502 Diagast] anti-H antibody [catalog no. 922102, BioLegend]; anti-Lewis<sup>a</sup> antibody [catalog no. 922202, BioLegend]; anti-Lewis<sup>b</sup> antibody [catalog no. SAB4700761, Sigma]; anti-Lewis<sup>x</sup> antibody [catalog no. 912901, BioLegend]; and anti-Lewis<sup>y</sup> antibody [catalog no. 912501, BioLegend]. After three washes, the plate was incubated for 1 h at 37°C with a secondary antibody at 1:2,000 with 1% BSA (anti-mouse HRP). After three washes, the reactions were developed with SigmaFast-OPD (Sigma), stopped with 2 M H<sub>2</sub>SO<sub>4</sub>, and read at 492 nm. Saliva from a Se+B individual<sup>48</sup> (secretor positive, which possesses at least one functional copy of the *FUT2* gene and thus synthesizes fucosylated HBGA with  $\alpha$ 1,2 linkages; blood group B) were used as controls to test functionality of the antibodies (Supplementary Figure S5). As a negative control, each well of bacteria was incubated with the secondary antibody (anti-mouse HRP) only.

### **Isolation of *Rhodococcus* spp. EPS**

To isolate the EPS from the five *Rhodococcus* spp. strains the protocol described by Wa *et al.*, 2022 was utilized with modifications.<sup>49</sup> Bacteria were cultured overnight in YEME medium at 30°C and agitation at 200 rpm. Next day the cells were pelleted and the supernatants were incubated with trichloroacetic acid at a final concentration of 20% (v/v) for 8 h at 4°C to precipitate the proteins. The samples were centrifuged at 12,000  $\times$  g and anhydrous ethanol with a ratio 3:1 (v/v) was added to the supernatants to precipitate the EPS. Samples were centrifuged at 12,000  $\times$  g for 20 min at 4°C and the pellet containing the EPS was diluted in 2 ml of ultrapure water. To quantify the EPSs the phenol/sulfuric method was used. 10  $\mu$ l of each sample was mixed 1:1 (v/v) with a solution of 6% phenol. Then, 100  $\mu$ l of concentrated sulfuric acid were added and the samples were incubated 30 min at room temperature. Absorbance at 480 nm was measured and the concentration was calculated using a calibration curve performed with known amounts of glucose.

The EPS from the strain *R. erythropolis* was biotinylated in one step as previously described.<sup>50</sup> In brief, 4,6 mg Biotin-LC-hydrazide (Pierce) was dissolved in 70  $\mu$ l of dimethyl sulfoxide (Sigma Aldrich) by vigorous mixing and heating at 65°C for 1 min. Afterwards, 30  $\mu$ l of glacial acetic acid were added and the mixture was poured onto 6.4 mg of cyanoborohydride (Sigma Aldrich) that was completely dissolved after heating at 65°C for 1 min. Then, the mixture was added to 1 mg of dried EPS. The reaction was carried out at 65°C for 2 h and the sample was purified immediately. A purification cartridge was prepared with two filter discs (12 mm in diameter) of Whatman QM-A Quartz Microfiber filters inserted in a holder (5-ml syringe). The cartridge was washed with 1 ml of water, 1 ml of 30% acetic acid in water, and 1 ml of acetonitrile. Then the sample was uniformly applied on top of the filters and allowed to bind for 15 min. The filters were washed with 1 ml of acetonitrile, 6  $\times$  1 ml with 4% acetonitrile in water and finally eluted in 4  $\times$  0.5 mL of water.

### **Binding assay of bacterial EPS with NoV GII.4 Sydney 2012 and NoV GII.6 VLP**

To demonstrate the specific binding of two different NoV genotypes (GII.4 Sydney 2012 and GII.6) and ELISA-like binding assay was established following the protocol described<sup>14</sup> with modifications. One  $\mu\text{g}$  per well in 100  $\mu\text{l}$  of each of the NoV VLP (VP1+VP2) or 1  $\mu\text{g}$  of RVA DLP (VP2+VP6) were coated in triplicate at 4°C overnight in carbonate/bicarbonate buffer. After three washes with 200  $\mu\text{l}$  of PBS-T, the plate was blocked for 1 h at 37°C with 200  $\mu\text{l}$  of 3% BSA in PBS-T. The wells were then incubated with 10  $\mu\text{g}$  per well of each one of the purified EPS (see above) and incubated at 37°C for 2 h. After three washes with 200  $\mu\text{l}$  of PBS-T, the plates were incubated with 100  $\mu\text{l}$ /well of anti-blood group B antibody (Diagast) diluted 1/100 in PBS-T and incubated for 1 h at 37°C. After three washes, the plate was incubated for 1 h at 37°C with a secondary antibody at 1:2,000 with PBS-T containing 1% BSA (anti-mouse HRP). After three washes, the reactions were developed with SigmaFast-OPD (Sigma), stopped with 2 M  $\text{H}_2\text{SO}_4$ , and read at 492 nm.

### **Binding blocking assay of bacterial EPS with NoV GII.4 Sydney 2012 and NoV GII.6 VLP**

The blocking ability of a combination of monoclonal anti-blood group A (catalog no. 70501 Diagast), and anti-blood group B antibodies (catalog no. 70502 Diagast) mixture was studied using the biotinylated EPS from the *R. erythropolis* strain. To study the blocking ability, NoV VLP as well as RVA DLP were coated in ELISA plates as described above. During the blocking step, a dilution 1/100 of both anti-A anti-B antibodies was incubated with the biotinylated EPS from *R. erythropolis* at a concentration of 10  $\mu\text{g}/\text{ml}$  in PBS. After this blocking step, the wells were washed and the blocked biotin-EPS, as well as a control without antibodies were added in triplicate (100  $\mu\text{l}$  per well). The ELISA plate was incubated 2 h at 37°C to allow EPS binding to VLP. After washing (3  $\times$  200  $\mu\text{l}$  of PBS-T), 100  $\mu\text{l}$  of a HRP-streptavidin (Sigma Aldrich) diluted 1/5,000 in PBS-T were added to each well and incubated 1 h at 37°C. After three washes, the reactions were developed

with SigmaFast-OPD (Sigma), stopped with 2 M  $\text{H}_2\text{SO}_4$ , and read at 492 nm.

### **Replication of GII.4 Sydney 2012 NoV in HIE in the presence of *R. erythropolis***

Secretor positive HIE derived from human jejunal biopsy (J2 cell line) were provided by Prof. Mary K. Estes (Baylor College of Medicine, Houston, TX). Undifferentiated 3D HIE and differentiated monolayers were maintained and produced using commercial IntestiCult™ Organoid Medium Human media (STEMCELL Technologies Inc.). HIE cultures were maintained and propagated as undifferentiated 3D cultures embedded in Matrigel using Organoid Growth Media (OGM), prepared by mixing equal volumes of components A and B, and supplemented with 10 mm ROCK inhibitor Y-27632. After 7 days, highly dense 3D cultures were dissociated into a single cell suspension and plated as undifferentiated monolayers. To this end, domes were broken and cells resuspended in Gentle Cell Dissociation Reagent (STEMCELL Technologies Inc.). After 10-min incubation on a rocking platform, dissociated cells were pelleted for 5 min at 200  $\times g$ , resuspended in OGM, and seeded onto a 96-well plate previously coated with collagen IV. After 24 h at 37°C in 5%  $\text{CO}_2$ , OGM was replaced with differentiation medium (ODM), to induce monolayer differentiation. ODM was prepared by mixing an equal volume of component A and CMGF-medium (consisted of advanced DMEM – F-12 medium supplemented with 100 U/ml penicillin-streptomycin, 10 mm HEPES buffer, and 1  $\times$  GlutaMAX). HIE cell monolayers resulted differentiated and 100% confluent after 5- to 2-days and used for NoV infections using a NoV GII.4 Sydney 2012 strain obtained from NoV diarrheal sample.

Three different infection experiments were carried out: (i) displacement (*R. erythropolis* ( $\text{OD}_{600} = 1$ ) inoculated after NoV GII.4 Sydney 2012;  $10^4$  genome equivalents per well); (ii) exclusion (*R. erythropolis* ( $\text{OD}_{600} = 1$ ) inoculated before NoV GII.4 Sydney 2012;  $10^4$  genome equivalents per well), and (iii) competitive exclusion (*R. erythropolis* ( $\text{OD}_{600} = 1$ ) and NoV GII.4 Sydney 2012,  $10^4$  genome equivalents per well, inoculated simultaneously). To this end, two sets

of 96-well plates with 100% confluent and differentiated HIE monolayers were inoculated in quadruplicate with 100 µl of each sample and incubated at 37°C for 2 h. Then, the inoculum was removed, monolayers were washed twice with CMGF-, and 100 µl of ODM was added to each well. For each set of infections, one 96-well plate was immediately frozen at −80°C (2 h post infection; hpi) and the second plate was incubated at 37°C and 5% CO<sub>2</sub> for 24 h (24 hpi) and then frozen. Finally, RT-qPCR was used to determine the amount of NoV RNA from HIE monolayers at 2 and 24 hpi to evaluate NoV replication.

### Quantification of GII.4 Sydney 2012 NoV replication in HIE

Viral RNA was extracted using the Maxwell® RSC Instrument (Promega) according to the manufacturer's instructions. Then, NoV RNA was detected in duplicate by TaqMan RT-qPCR using the RNA UltraSense One-Step quantitative RT-PCR system (Invitrogen) on a LightCycler 480 instrument (Roche Diagnostics, Germany). The set of primers and probe included in the ISO 15,216–1 (2017) was used for detecting NoV GII.4 Sydney.

Tenfold serial dilutions of synthetic gBlock gene fragments (IDT) were included to quantify the NoV RNA into genome equivalents (NoV GII.4:  $y = -3.56 \times +40.664$ ,  $R = 0.997$ ). Positive and negative amplification controls were included in each run. To report NoV replication (R), results were presented as RNA fold increase, calculated as:

$$R = C_{24\text{hpi}}/C_{2\text{hpi}}$$

where  $R$  = RNA fold increase;  $C_{24\text{hpi}}$  = NoV titer at 24 hpi (genome copies/100 µl);  $C_{2\text{hpi}}$  = NoV titer at 2 hpi (genome copies/100 µl).

### Toxicity assay

A toxicity assay was performed to assess how the *R. erythropolis* affect HIE viability at different doses ( $\text{OD}_{600} = 0.5$ ,  $\text{OD}_{600} = 1$  and  $\text{OD}_{600} = 2$ ). HIE were incubated with the different concentrations of bacteria for 2 h as described above, but excluding the viral infection. After the incubation with

*R. erythropolis* the cells were followed up for 24 h inspecting the monolayer integrity at 1, 3, 18 and 24 h. Monolayer integrity was calculated as the fraction of cell area (analyzing the cell membrane refringence) versus total well area using ImageJ2 (version 2.14.0/1.54f).

### Statistical analyses

To assess the statistical differences between the different groups GraphPad software (GraphPad Prism version 9.0 for MacOSx) was utilized applying the one-way ANOVA test when multiple groups were compared and the Student's *t*-test to assess differences between two groups. Differences were considered significative when the *p*-value was <0.05.

### Disclosure statement

No potential conflict of interest was reported by the author(s).

### Funding

This work was supported by the Spanish Ministry of Science and Innovation (MICIN)/Spanish State Research Agency (AEI)/10.13039/501100011033 under Grant [PID2020-115403RB-C21] to M.J.Y., PID2020-115403RB-C22 to J.R.-D., and PID2019-105509RJ-I00 to W.R. The study was also supported by Valencian Government grant AICO/2021/033 to J.R.-D. C.S.-B. and S.L.-N. are recipients of the FPI PRE2018-083315 and FPU22/00443 predoctoral grants by MICIN/AEI/10.13039/501100011033 and by "ESF Investing in your future". N.P.-G., R.C.-C., and N.N.-L. are recipients of predoctoral grants from the Valencian Government (ACIF/2020/085, CIACIF/2021/162 and ACIF/2020/076).

### ORCID

Cristina Santiso-Bellón  <http://orcid.org/0000-0003-1698-5062>

Walter Randazzo  <http://orcid.org/0000-0002-7433-149X>

Nazaret Peña-Gil  <http://orcid.org/0000-0003-3553-4582>

Roberto Cárcamo-Calvo  <http://orcid.org/0000-0003-4753-7406>

Sergi Lopez-Navarro  <http://orcid.org/0000-0002-1893-2776>

Noemi Navarro-Lleó  <http://orcid.org/0000-0003-2572-9220>

Maria J. Yebra  <http://orcid.org/0000-0003-4638-986X>

Vicente Monedero  <http://orcid.org/0000-0001-7461-8047>

Javier Buesa  <http://orcid.org/0000-0002-3328-3428>

Roberto Gozalbo-Rovira  <http://orcid.org/0000-0003-3427-3800>

Jesús Rodríguez-Díaz  <http://orcid.org/0000-0002-9698-7684>

## Data availability statement

The raw sequencing fastq files were deposited in the SRA repository (<http://www.ncbi.nlm.nih.gov/sra> accessed 30 July 2024) under Bioproject ID PRJNA706108, SRA from SRX17673803 to SRX17673838.

## Ethics statement

All experiments using mice were conducted at the Animal Production and Experimentation Service of the University of Valencia following national and international regulations. The procedures were approved by Ethics Committee for Animal Welfare and by the “Dirección General de Agricultura, Ganadería y Pesca” of the “Generalitat Valenciana”, file number 2018/VSC/PEA/0181 approved on 19 December 2018. Use of human stool samples was approved by the Human Research Ethics Committee of the University of Valencia (registration number H154401046838).

## References

- World Health Organization (WHO). The top 10 causes of death [Internet]. 2020 [accessed 2023 June 19]. <https://www.who.int/news-room/fact-sheets/detail/the-top-10-causes-of-death>.
- Centers for Disease Control and Prevention (CDC). Norovirus Burden and Trends [Internet]. 2023 [accessed 2023 June 19]. <https://www.cdc.gov/norovirus/burden.html#worldwide>.
- Bucardo F, Lindgren PE, Svensson L, Nordgren J, Sestak K. Low prevalence of rotavirus and high prevalence of norovirus in hospital and community wastewater after introduction of rotavirus vaccine in Nicaragua. *PLOS ONE*. 2011;6(10):6. doi:10.1371/journal.pone.0025962.
- Patel MM, Hall AJ, Vinjé J, Parashar UD. Noroviruses: a comprehensive review. *J Clin*. 2009;44(1):1–8. doi:10.1016/j.jcv.2008.10.009.
- Donaldson EF, Lindesmith LC, Lobue AD, Baric RS. Norovirus pathogenesis: mechanisms of persistence and immune evasion in human populations. *Immunological Rev*. 2008;225(1):190–211. doi:10.1111/j.1600-065X.2008.00680.x.
- Chhabra P, de Graaf M, Parra GI, Chan MCW, Green K, Martella V, Wang Q, White PA, Katayama K, Vennema H, et al. Updated classification of norovirus genogroups and genotypes. *J Gen Virol*. 2019;100(10):1393–1406. doi:10.1099/jgv.0.001318.
- Cao S, Lou Z, Tan M, Chen Y, Liu Y, Zhang Z, Zhang XC, Jiang X, Li X, Rao Z. Structural basis for the recognition of blood group trisaccharides by norovirus. *J Virol*. 2007;81(11):5949–5957. doi:10.1128/JVI.00219-07.
- Huang P, Farkas T, Zhong W, Tan M, Thornton S, Morrow AL, Jiang X. Norovirus and histo-blood group antigens: demonstration of a wide spectrum of strain specificities and classification of two major binding groups among multiple binding patterns. *J Virol*. 2005;79(11):6714–6722. doi:10.1128/JVI.79.11.6714-6722.2005.
- Shanker S, Choi J-M, Sankaran B, Atmar RL, Estes MK, Prasad BVV. Structural analysis of histo-blood group antigen binding specificity in a norovirus GII.4 epidemic variant: implications for epochal evolution. *J Virol*. 2011;85(17):8635–8645. doi:10.1128/JVI.00848-11.
- Tan M, Jiang X. Histo-blood group antigens: a common niche for norovirus and rotavirus. *Expert Rev Mol Med [Internet]*. 2014;16:e5. <https://www.cambridge.org/core/journals/expert-reviews-in-molecular-medicine/article/abs/histoblood-group-antigens-a-common-niche-for-norovirus-and-rotavirus/4F5EF25524DCF746E7EA921E6A56D4BD>.
- Monedero V, Buesa J, Rodríguez-Díaz J. The interactions between host glycobiology, bacterial microbiota, and viruses in the gut. *Viruses*. 2018;10(2):1–14. doi:10.3390/v10020096.
- Peña-Gil N, Santiso-Bellón C, Gozalbo-Rovira R, Buesa J, Monedero V, Rodríguez-Díaz J. The role of host glycobiology and gut microbiota in rotavirus and norovirus infection, an update. *Int J Mol Sci*. 2021;22(24):13473. doi:10.3390/ijms222413473.
- Santiso-Bellón C, Gozalbo-Rovira R, Buesa J, Rubio-Del-Campo A, Peña-Gil N, Navarro-Lleó N, Cárcamo-Calvo R, Yebra MJ, Monedero V, Rodríguez-Díaz J. Replication of human norovirus in mice after antibiotic-mediated intestinal bacteria depletion. *Int J Mol Sci*. 2022;23(18):10643. doi:10.3390/ijms231810643.
- Miura T, Sano D, Suenaga A, Yoshimura T, Fuzawa M, Nakagomi T, Nakagomi O, Okabe S. Histo-blood group antigen-like substances of human enteric bacteria as specific adsorbents for human noroviruses. *J Virol*. 2013;87(17):9441–9451. doi:10.1128/JVI.01060-13.
- Almand EA, Moore MD, Jaykus LA. Characterization of human norovirus binding to gut-associated bacterial ligands. *BMC Res Notes*. 2019;12(1):607. doi:10.1186/s13104-019-4669-2.
- Gozalbo-Rovira R, Rubio-Del-Campo A, Santiso-Bellón C, Vila-Vicent S, Buesa J, Delgado S, Molinero N, Margolles A, Yebra MJ, Collado MC, et al. Interaction of intestinal bacteria with human rotavirus during infection in children. *Int J Mol Sci*. 2021;22(3):1010–1012. doi:10.3390/ijms22031010.



17. Almand EA, Moore MD, Outlaw J, Jaykus L-A, Calderaro A. Human norovirus binding to select bacteria representative of the human gut microbiota. *PLOS ONE*. 2017;12(3):e0173124. doi:10.1371/journal.pone.0173124.
18. Urai M, Yoshizaki H, Anzai H, Ogihara J, Iwabuchi N, Harayama S, Sunairi M, Nakajima M. Structural analysis of an acidic, fatty acid ester-bonded extracellular polysaccharide produced by a pristane-assimilating marine bacterium, *Rhodococcus erythropolis* PR4. *Carbohydr Res*. 2007;342(7):933–942. doi:10.1016/j.carres.2007.02.001.
19. Gozalbo-Rovira R, Ciges-Tomas JR, Vila-Vicent S, Buesa J, Santiso-Bellón C, Monedero V, Yebra MJ, Marina A, Rodríguez-Díaz J, Rey FA. Unraveling the role of the secretor antigen in human rotavirus attachment to histo-blood group antigens. *PLOS Pathog* [Internet]. 2019;15(6):e1007865. doi:10.1371/journal.ppat.1007865.
20. Kuss SK, Best GT, Etheredge CA, Pruijssers AJ, Frierson JM, Hooper LV, Dermody TS, Pfeiffer JK. Intestinal microbiota promote enteric virus replication and systemic pathogenesis. *Sci* (1979). 2011;334(6053):249–252. doi:10.1126/science.1211057.
21. Kane M, Case LK, Kopaskie K, Kozlova A, MacDermid C, Chervonsky AV, Golovkina TV. Successful transmission of a retrovirus depends on the commensal microbiota. *Sci* (1979). 2011;334(6053):245–249. doi:10.1126/science.1210718.
22. Monedero V, Collado MC, Rodríguez-Díaz J. Therapeutic opportunities in intestinal microbiota–virus interactions. *Trends Biotechnol*. 2018;36(7):645–648. doi:10.1016/j.tibtech.2017.12.009.
23. Kim AHJ, Hogarty MP, Harris VC, Baldrige MT. The complex interactions between rotavirus and the gut microbiota. *Front Cell Infect Microbiol*. 2021;10. doi:10.3389/fcimb.2020.586751.
24. Roth AN, Grau KR, Karst SM. Diverse mechanisms underlie enhancement of enteric viruses by the mammalian intestinal microbiota. *Viruses*. 2019;11(8):11. doi:10.3390/v11080760.
25. Liao N, Tang M, Chen L, Tian P, Wang D, Cheng D, Wu G. Soluble extracellular polymeric substance (SEPS) of histo-blood group antigen (HBGA) expressing bacterium *Sphingobacterium* sp. SC015 influences the survival and persistence of norovirus on lettuce. *Food Microbiol*. 2023;109:104126. doi:10.1016/j.fm.2022.104126.
26. Garrido-Sanz D, Redondo-Nieto M, Martín M, Rivilla R. Comparative genomics of the rhodococcus genus shows wide distribution of biodegradation traits. *Microorganisms*. 2020;8(5):8. doi:10.3390/microorganisms8050774.
27. Martínková L, Uhnáková B, Pátek M, Nešvera J, Křen V. Biodegradation potential of the genus *Rhodococcus*. *Environ Int*. 2009;35(1):162–177. doi:10.1016/j.envint.2008.07.018.
28. Lin X, Abdalla M, Yang J, Liu L, Fu Y, Zhang Y, Yang S, Yu H, Ge Y, Zhang S, et al. Relationship between gut microbiota dysbiosis and immune indicator in children with sepsis. *BMC Pediatr* [Internet]. 2023;23(1):1–10. doi:10.1186/s12887-023-04349-8.
29. Ma L, Yan Y, Webb RJ, Li Y, Mehrabani S, Xin B, Sun X, Wang Y, Mazidi M. Psychological stress and gut microbiota composition: a systematic review of human studies. *Neuropsychobiol* [Internet]. 2023;82(5):247–262. doi:10.1159/000533131.
30. Lin PC, Ycsh Y, Lin SC, Lu MC, Tsai YT, Lu SC, Chen SH, Chen SY, Calderaro A. Clinical significance and intestinal microbiota composition in immunocompromised children with norovirus gastroenteritis. *PLOS ONE*. 2022;17(4):17. doi:10.1371/journal.pone.0266876.
31. Rubio-Del-Campo A, Coll-Marqués JM, Yebra MJ, Buesa J, Pérez-Martínez G, Monedero V, Rodríguez-Díaz J, Sestak K. Noroviral P-particles as an in vitro model to assess the interactions of noroviruses with probiotics. *PLOS ONE*. 2014;9(2):e89586. doi:10.1371/journal.pone.0089586.
32. Perry MB, MacLean LL, Patrauchan MA, Vinogradov E. The structure of the exocellular polysaccharide produced by *Rhodococcus* sp. RHA1. *Carbohydr Res*. 2007;342(15):2223–2229. doi:10.1016/j.carres.2007.07.002.
33. Hu X, Li D, Qiao Y, Wang X, Zhang Q, Zhao W, Huang L. Purification, characterization and anticancer activities of exopolysaccharide produced by *Rhodococcus erythropolis* HX-2. *Int J Biol Macromol*. 2020;145:646–654. doi:10.1016/j.ijbiomac.2019.12.228.
34. De Graaf M, Van Beek J, Koopmans MPG. Human norovirus transmission and evolution in a changing world. *Nat Rev Microbiol*. 2016;14(7):421–433. doi:10.1038/nrmicro.2016.48.
35. Yu Y, Han F, Yang M, Zhang X, Chen Y, Yu M, Wang Y. *Pseudomonas composti* isolate from oyster digestive tissue specifically binds with norovirus GII.6 via Psl extracellular polysaccharide. *Int J Food Microbiol*. 2023;406:110369. doi:10.1016/j.ijfoodmicro.2023.110369.
36. Gimeno A, Delgado S, Valverde P, Bertuzzi S, Berbis MA, Echavarren J, Lacetera A, Martín-Santamaría S, Suroli A, Cañada FJ, et al. Minimizing the entropy penalty for ligand binding: lessons from the molecular recognition of the histo blood-group antigens by human galectin-3. *Angew Chem Int Ed*. 2019;58(22):7268–7272. doi:10.1002/anie.201900723.
37. Palm E, Danskog K, Nord S, Becker M, Tanner H, Sandblad L, Öhlund D, Lenman A, Arnberg N. Bile acids accumulate norovirus-like particles and enhance binding to and entry into human enteric epithelial cells. *bioRxiv* [Internet]. 2023; 2023.04.28.538707. <http://biorxiv.org/content/early/2023/05/01/2023.04.28.538707.abstract>.



38. Robinson CM, Jesudhasan PR, Pfeiffer JK. Bacterial lipopolysaccharide binding enhances virion stability and promotes environmental fitness of an enteric virus. *Cell Host Microbe*. 2014;15(1):36–46. doi:10.1016/j.chom.2013.12.004.
39. Guo CT, Ohta S, Yoshimoto A, Nakata K, Shortridge KF, Takahashi T, Suzuki T, Miyamoto D, Jwa Hidari KIP, Suzuki Y. A unique phosphatidylinositol bearing a novel branched-chain fatty acid from *Rhodococcus equi* binds to influenza virus hemagglutinin and inhibits the infection of cells. *J Biochem*. 2001;130(3):377–384. doi:10.1093/oxfordjournals.jbchem.a002996.
40. Jones MK, Watanabe M, Zhu S, Graves CL, Keyes LR, Grau KR, Gonzalez-Hernandez MB, Iovine NM, Wobus CE, Vinjé J, et al. Enteric bacteria promote human and mouse norovirus infection of B cells. *Sci* (1979). 2014;346(6210):755–759. doi:10.1126/science.1257147.
41. Lei S, Samuel H, Twitchell E, Bui T, Ramesh A, Wen K, Weiss M, Li G, Yang X, Jiang X, et al. *Enterobacter cloacae* inhibits human norovirus infectivity in gnotobiotic pigs. *Sci Rep*. 2016;6(1):6. doi:10.1038/srep25017.
42. Kojima S, Kageyama T, Fukushi S, Hoshino FB, Shinohara M, Uchida K, Natori K, Takeda N, Katayama K. Genogroup-specific PCR primers for detection of Norwalk-like viruses. *J Virol Methods*. 2002;100(1–2):107–114. doi:10.1016/S0166-0934(01)00404-9.
43. Buesa J, Collado B, López-Andújar P, Abu-Mallouh R, Rodríguez Díaz J, García Díaz A, Prat J, Guix S, Llovet T, Prats G, et al. Molecular epidemiology of caliciviruses causing outbreaks and sporadic cases of acute gastroenteritis in Spain. *J Clin Microbiol*. 2002;40(8):2854–2859. doi:10.1128/JCM.40.8.2854-2859.2002.
44. Beuret C, Kohler D, Baumgartner A, Lüthi TM. Norwalk-like virus sequences in mineral waters: one-year monitoring of three brands. *Appl Environ Microbiol*. 2002;68(4):1925–1931. doi:10.1128/AEM.68.4.1925-1931.2002.
45. Madrigal JL, Jones MK. Quantifying human norovirus virus-like particles binding to commensal bacteria using flow cytometry. *J Visualized Experiments*. 2020; (158):2020. doi:10.3791/61048.
46. Dhariwal A, Chong J, Habib S, King IL, Agellon LB, Xia J. Microbiomeanalyst: a web-based tool for comprehensive statistical, visual and meta-analysis of microbiome data. *Nucleic Acids Res*. 2017;45(W1):W180–W188. doi:10.1093/nar/gkx295.
47. Segata N, Izard J, Waldron L, Gevers D, Miropolsky L, Garrett WS, Huttenhower C. Metagenomic biomarker discovery and explanation. *Genome Biol* [Internet]. 2011;12(6):1–18. doi:10.1186/gb-2011-12-6-r60.
48. Rodríguez-Díaz J, García-Mantrana I, Vila-Vicent S, Gozalbo-Rovira R, Buesa J, Monedero V, Collado MC. Relevance of secretor status genotype and microbiota composition in susceptibility to rotavirus and norovirus infections in humans. *Sci Rep*. 2017;7:45559. doi:10.1038/srep45559.
49. Wa Y, Chanyi RM, Nguyen HTH, Gu R, Day L, Altermann E, Cocolin L. Extracellular polysaccharide extraction from *Streptococcus thermophilus* in fermented milk. *Microbiol Spectr* [Internet]. 2022;10(2). doi:10.1128/spectrum.02280-21.
50. Grün CH, van Vliet SJ, Schiphorst WECM, Bank CMC, Meyer S, van Die I, van Kooyk Y. One-step biotinylation procedure for carbohydrates to study carbohydrate–protein interactions. *Anal Biochem*. 2006;354(1):54–63. doi:10.1016/j.ab.2006.03.055.